Proc. Natl. Acad. Sci. USA
Vol. 85, pp. 8311–8315, November 1988
Neurobiology

Axonal delay lines for time measurement in the owl's brainstem

(sound localization/auditory system/nucleus laminaris/neural map/*Tyto alba*)

CATHERINE E. CARR* AND MASAKAZU KONISHI

Division of Biology, 216-76, California Institute of Technology, Pasadena, CA 91125

Contributed by Masakazu Konishi, July 15, 1988

ABSTRACT **Interaural time difference is an important cue for sound localization. In the barn owl (*Tyto alba*) neuronal sensitivity to this disparity originates in the brainstem nucleus laminaris. Afferents from the ipsilateral and contralateral magnocellular cochlear nuclei enter the nucleus laminaris through its dorsal and ventral surfaces, respectively, and interdigitate in the nucleus. Intracellular recordings from these afferents show orderly changes in conduction delay with depth in the nucleus. These changes are comparable to the range of interaural time differences available to the owl. Thus, these afferent axons act as delay lines and provide anatomical and physiological bases for a neuronal map of interaural time differences in the nucleus laminaris.**

Jeffress (1) proposed a model, the place theory, for measurement of the interaural time differences that underlie sound localization. His theory contained two important concepts, the first being the principles of delay lines and coincidence detection. The second states that the "place" or anatomical location of the neuron in an array encodes the place or location of the sound. In the model, the coincidence detectors are binaural neurons which require simultaneous arrival of spikes from the two sides to elicit a maximal discharge. Signals reach these coincidence detectors by axonal paths which are unequal for the two sides. This difference in path lengths translates into a disparity in spike conduction time. The coincidence detectors respond preferentially to an interaural time difference that delays the arrival of spikes on the shorter path, and advances the arrival of spikes on the longer path so as to cause the spikes to arrive simultaneously. Subsequently, several authors proposed cross-correlation models of sound localization using the same principles (2, 3). Goldberg and Brown (4), working on the superior olive of dogs, obtained data consistent with the Jeffress model, and similar results have been obtained in cats (5).

Barn owls use interaural time differences to localize sound in azimuth (6). Neuronal sensitivity to these time differences arises in the nucleus laminaris (7), the avian homologue of the medial superior olive. As in the superior olive, physiological responses from nucleus laminaris are consistent with the principles of the Jeffress model (8).

Despite the widespread acceptance of the Jeffress model, the nature of the delay lines and the cellular mechanisms of coincidence detection remain to be investigated. Conduction delays can be produced by several different methods, such as variation in membrane time constants, number of synapses, length of dendrites, and length of axonal path (9, 10). We present both anatomical and physiological evidence for axonal delay lines in the barn owl's nucleus laminaris.

MATERIALS AND METHODS

Anatomy. Horseradish peroxidase (HRP) was used as a tracer to study the innervation of nucleus laminaris in five owls (*Tyto alba*) (11). Detailed protocols may be found in ref. 12. Birds were anesthetized by intramuscular (i.m.) injection of ketamine hydrochloride (4 mg/kg per hr, Vetalar, Bristol Laboratories, Syracuse, NY), and the skull was immobilized. After a craniotomy, the nucleus magnocellularis was stereotaxically and physiologically identified. HRP was then injected extracellularly with a glass pipette of 20–40 μm diameter. HRP (Boehringer Mannheim) was prepared in filtered 0.5 M KCl/Tris·HCl buffer at pH 7.6 and iontophoresed with 2-μA pulsed positive current for 5–10 min. Sufficient neural activity may be recorded through these electrodes to identify the best frequency of the recording site. After several days of survival, animals were anesthetized with ketamine (4 mg/kg i.m.) followed by an overdose of Nembutal (100 mg/kg i.m.), then perfused transcardially with normal saline, followed immediately by 1 liter of 1.25% glutaraldehyde/2% paraformaldehyde in 0.1 M sodium phosphate buffer at pH 7.2. The brain was postfixed overnight at 4°C, sectioned in cold pH 7.2 phosphate buffer with a vibratome, and allowed to react with diaminobenzidine as a chromagen. Several of the best-labeled fibers were reconstructed in each case by the method of Sereno (13). The tonotopic organization of the nucleus magnocellularis resulted in labeled fibers traveling together. Discrimination between these fibers was based on accurate reconstructions at high magnification. We obtained labeling of an entire arbor only from extracellular injections; complete labeling was never obtained from intracellular HRP injections.

Physiology. For neurophysiological recording, birds were anesthetized as above, and the skull was immobilized. The floor of the fourth ventricle was exposed by removal of the overlying cerebellum. All data had to be obtained by intracellular methods, because extracellular signals were masked by overwhelming field potentials, termed the neurophonic (8). A World Precision Instruments (New Haven, CT) M701 electrometer recorded action potentials, which were amplified, filtered, and level-discriminated by an ac amplifier. A PDP11/40 computer recorded the time of occurrence of computer-compatible pulses triggered by the level-discriminated spikes. The best frequency of each neuron was determined with the aid of an audio monitor. Whenever necessary, these measures of best frequency were confirmed by analyzing selected neurons with the aid of an automatic tuning program. Earphones inserted in the external meatus delivered tone bursts 300 msec in duration with a rise and decay time of 5 msec. The earphone assembly contained a Knowles "subminiature" probe microphone for the calibration of amplitude and phase near the eardrum. The phase response of the two earphones did not differ by more than 5 μsec over the frequency range used. Stimulus amplitude was approximately 40 decibels re 0.0002 μbar sound pressure level in all tests.

Measurement of Conduction Delay. Magnocellular afferents phase-lock, discharging at a particular phase angle of a sinu-

The publication costs of this article were defrayed in part by page charge payment. This article must therefore be hereby marked "*advertisement*" in accordance with 18 U.S.C. §1734 solely to indicate this fact.

Abbreviation: HRP, horseradish peroxidase.

*Present address: Department of Neurobiology and Anatomy, University of Rochester, 601 Elmwood Avenue, Rochester, NY 14642.

soidal stimulus (14). Shifts in the phase angle indicate changes in conduction time. Such shifts can be measured in period histograms, which show the probability of an action potential occurring at different phase angles during each tonal period. The degree of phase-locking, the vector strength, and the mean phase were calculated by the method of Goldberg and Brown (4). Mean phase values were used in analysis only if their vector strength values were greater than 0.2. Each period histogram constituted a response to 30,000 stimulus cycles and contained between 500 and 2500 spikes. Conduction delays in the nucleus laminaris were calculated in two different ways. The first method used the relationship phase = time × frequency, by which conduction time can be calculated from the slope of the phase–frequency plot (14). Only slopes with a correlation coefficient greater than 0.98 were used. Since this method required period histograms for four or more different frequencies for each neuron, it was time-consuming and could not be used in most recordings. The second method used only one stimulus frequency for all neurons recorded during one penetration. This method eliminated the effects of errors in the determination of best frequency on the measurement of mean phase. The method also enabled us to collect a large amount of phase data for selected frequencies so that the patterns of phase shifts might be compared among neurons recorded in different penetrations. These phase values were plotted against depth, and regression lines were drawn for data from both the ipsi- and contralateral afferents. All regression lines had correlation coefficients greater than 0.75. The slope of the regression line was expressed in degrees/μm. Conduction velocity (μm/μsec) was derived from change in mean phase with depth by conversion of phase to time (e.g., 360° at 5.5 kHz = 180 μsec). Conduction delay (μsec) over the 700-μm depth of the nucleus laminaris was then calculated. Conduction delays were determined for penetrations in the 5–7.5 kHz region and calculated from the slope of each plot (see Fig. 3). Only penetrations with at least 5 (mean = 10) separate intracellular recordings within nucleus laminaris were used in each calculation of delay. Data were obtained in seven owls and for six different frequencies; 4.5 kHz(n = 1), 5.0 kHz (n = 3), 5.5 kHz (n = 8), 6.0 kHz (n = 4), 6.5 kHz (n = 2), 7.0 kHz (n = 3), and 7.5 kHz (n = 2) (n = number of penetrations).

RESULTS

The cochlear nucleus magnocellularis projects bilaterally to the nucleus laminaris as in other birds (15–19). This projection is tonotopic, as demonstrated by injections of tritiated proline into the nucleus magnocellularis (12). In the barn owl, the nucleus laminaris is a hypertrophied nucleus situated on the floor of the fourth ventricle, bordered on its dorsal surface by a thick fiber layer which consists of a superficial layer of eighth nerve axons and a deeper layer of afferents from the ipsilateral nucleus magnocellularis. The nucleus laminaris is bordered on its ventral surface by afferents from the contralateral nucleus magnocellularis. These two fiber layers sandwich the neuropil of the nucleus, which is made up of a single neuronal cell type and afferents from the two cochlear nuclei. Axons from the ipsilateral nucleus magnocellularis travel along the dorsal border of the nucleus laminaris, while axons from the contralateral nucleus magnocellularis travel along the ventral border until they reach their specific isofrequency band. There, each axon gives off collaterals that enter the nucleus laminaris (Fig. 1). The ipsi- and contralateral axons appear to contact the sparsely distributed laminaris somata both *en passant* and as terminal boutons.

If these afferents act as delay lines, physiological recordings should show an orderly change in conduction delay along the axons. For this reason, the nucleus laminaris was penetrated perpendicular to its dorsal and ventral surfaces, and hence roughly parallel to the incoming axons. Sampling of axons during each penetration therefore was confined to a

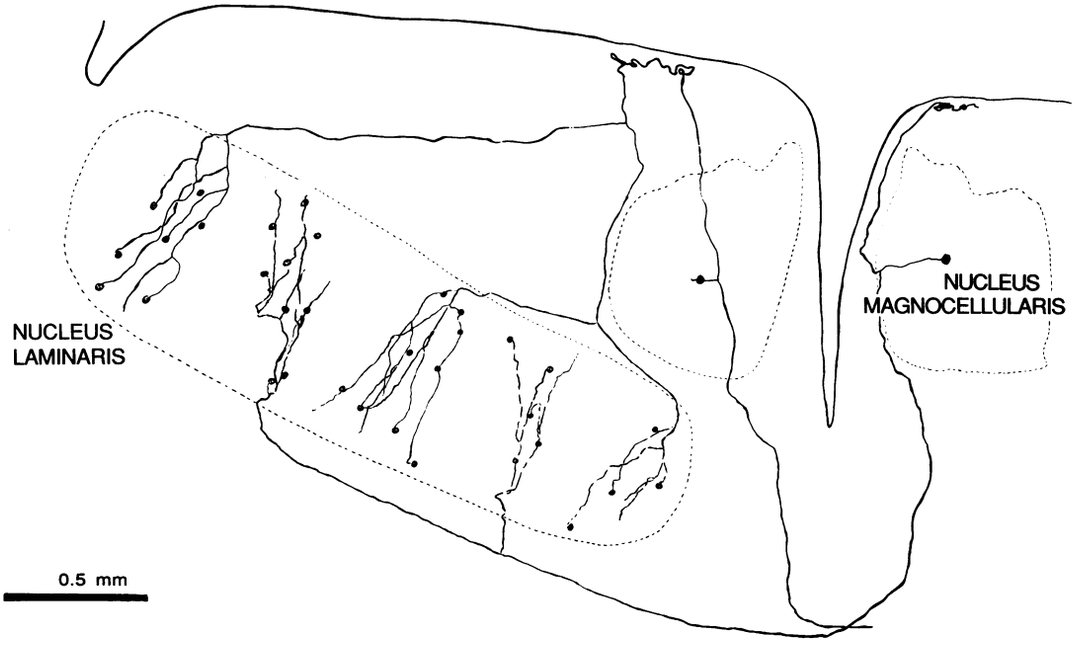

FIG. 1. Projection of magnocellularis afferents to nucleus laminaris. The nucleus magnocellularis projects bilaterally to the nucleus laminaris, such that afferents from the two sides interdigitate in a counter-current fashion within the nucleus. Magnocellular neurons were labeled after small HRP injections into the 5.5-kHz region of either the left or the right nucleus in two owls. The ipsilateral arbor of one cell and the contralateral arbor of another were reconstructed and combined in the same figure. The nucleus laminaris is organized in diagonal frequency bands that run from caudomedial to rostrolateral; thus the most medial fibers are also the most caudal. Each axon travels rostrolaterally along the edge of the nucleus, giving off collaterals at regular intervals. Laminaris neurons are sparsely distributed throughout the nucleus; each neuron close enough to a labeled fiber to be a candidate for synaptic input is shown. The plane of this figure is a transverse slab, and this reconstruction is based on about twenty 100-μm sections. A preliminary version of this figure has already been published (20).

single bundle of afferents having the same or similar best frequencies. The dorsal and ventral surfaces of the nucleus laminaris were recognizable by distance from the floor of the fourth ventricle. The measurement of distance was confirmed by the deposition of HRP markers at or near the surfaces of the nucleus laminaris. In three owls, a penetration with an HRP-containing electrode followed the track of the previous intracellular recording electrode, and small amounts of HRP were injected at a depth of 800 μm and 1500 μm from the floor of the fourth ventricle. In all cases, label was found to the dorsal and ventral surfaces of the nucleus laminaris.

The order in which magnocellular afferents were encountered reflected the anatomical organization described above. Responses to stimulation of the ipsilateral ear alone were confined to the zone between the floor of the fourth ventricle and the dorsal surface of the nucleus laminaris. When the electrode entered the nucleus laminaris (at depth of about 800 μm from the floor of the fourth ventricle) responses to stimulation of the ipsi- or contralateral ear began to occur with equal probability. At the ventral surface of the nucleus laminaris (about 1500 μm deep) responses to stimulation of the ipsilateral ear were no longer obtained. Thus the dorsal and ventral borders of the nucleus were physiologically recognizable.

Since magnocellular fibers phase-lock, we were able to use period histograms to measure conduction time at different depths of the nucleus laminaris. As an electrode advanced through the nucleus laminaris, we recorded from ipsilateral and contralateral afferents. In either afferent we observed monotonic changes of mean phase interrupted by sudden shifts of phase angle, for example from 70° to 350° (Fig. 2*A*). Since phase (θ) is measured modulo 2π, we have made the assumption that the monotonic changes in phase with depth occur within a single stimulus cycle, and that a sudden shift in phase angle represents a crossover to the next cycle ($2\pi + \theta$) (Fig. 2*B*). We confirmed this assumption by determining the maximum difference in conduction time between the dorsal and ventral surfaces of the nucleus laminaris. Conduction time was measured between the ear and nucleus laminaris in two owls and in seven penetrations. The median

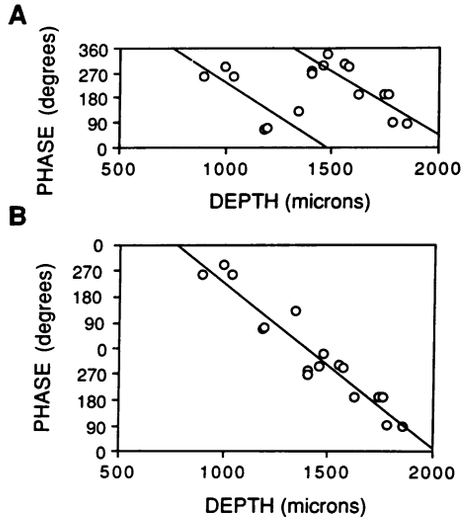

FIG. 2. Interpretation of sudden phase shifts. (*A*) Mean phase angles of contralateral fibers recorded at different depths during one penetration through the 7.0-kHz region are plotted within a single stimulus period. Monotonic changes in phase with depth are interrupted by a sudden shift around zero degree, forming a sawtooth shape. (*B*) These sawtooth-shaped plots have very similar slopes (−0.46 and −0.49 degree/μm, respectively). They were "unwrapped" to form a single plot of depth against phase for data analysis.

conduction time for ipsilateral fibers near the dorsal border of nucleus laminaris was 2.7 msec (n = 16 fibers) and near the ventral border it was 2.9 msec (n = 9). Median conduction times for contralateral fibers were 2.9 msec (n = 15) near the ventral portion of the nucleus laminaris, and 3.1 msec (n = 9) near the dorsal border. Dorsal and ventral conduction times for both ipsilateral and contralateral fibers were different at $p < 0.01$ level (Mann–Whitney U test). Thus the median conduction time from either the ipsilateral or the contralateral ear differed by about 200 μsec between the dorsal and ventral borders of the nucleus. Since this time difference is less than two periods of stimuli used (4.5–7.5 kHz), a sudden shift during monotonic phase changes should not involve more than one cycle, thus confirming our assumption.

We measured mean phase angles from 352 intracellular recordings from afferents within the nucleus laminaris in seven owls. Fig. 3 shows representative penetrations in which the mean phase of neurons varies with recording depth. Penetrations in the 5.5-kHz region of the nucleus laminaris show a gradual increase in phase with depth for afferents from the ipsilateral nucleus magnocellularis (Fig. 3*A*). The conduction delay for ipsilateral and contralateral afferents in the nucleus laminaris was calculated from the slope of each graph for every penetration. Although most penetrations in Fig. 3 were made in different animals, all show very similar changes in delay with depth. Recordings from contralateral afferents show similar but opposite changes in delay with depth (Fig. 3*B*). Figure 3*C* shows a single penetration through the 6.0 kHz region of the nucleus laminaris. At the dorsal surface (815 μm), ipsi- and contralateral axons were found within 50 μm of each other. Axons from both sides were encountered almost in alternation until the last ipsilateral axon was recorded at a depth of 1605 μm. Over this distance of 790 μm, mean phase on the ipsilateral path increased with depth from 180° to 2π + 180°. This phase shift corresponds to a change of 150 μsec over 700 μm. On the contralateral path, mean phase decreased with depth, from 2π + 180° at 885 μm to 90° at 1540 μm, a change of about 200 μsec over 700 μm.

Delays of phase-locked spikes, as measured in Fig. 3, varied systematically with depth in all isofrequency planes. We sampled neurons tuned to frequencies between 4.5 and 7.5 kHz and found similar patterns of change in delay with depth; the same range of delays occurs at roughly the same depth for all frequencies. This is most clearly illustrated by the point of intersection between the ipsilateral and contralateral plots of phase. At this depth, delays from the two ears are equal (Fig. 3*C*). This point was designated as zero phase difference to conform with the neurophonic map obtained in the owl (8). For all frequencies examined (4.5–7.5 kHz), this zero point was found at the same depth (mean ± SD = 1317 ± 61 μm, n = 8 penetrations). Similarly, the maximal delay was similar for all frequencies examined. Calculations show a delay of about 135 μsec over 700 μm for the ipsilateral path (mean delay = 137 ± 27 μsec, n = 13 penetrations), and 130 μsec over 700 μm for the contralateral path (mean delay = 129 ± 26 μsec, n = 16 penetrations). These delays are the same order of magnitude as the observed 200-μsec differences in conduction time between the dorsal and ventral surfaces of the nucleus laminaris.

DISCUSSION

Analysis of phase-locked field potentials (8) showed an orderly distribution of conduction delay along the dorsoventral axis of the nucleus laminaris. Conduction delay increased with recording depth for ipsilateral stimulation and decreased for contralateral stimulation, resulting in unequal ipsi- and contralateral delays at most depths. Furthermore, the depth at which a given delay occurred was constant across different

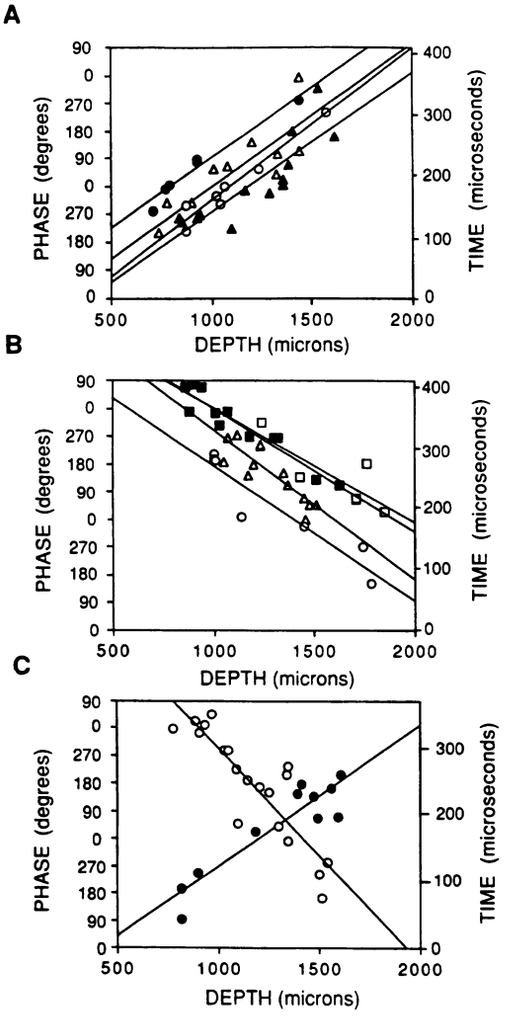

FIG. 3. Systematic changes in mean phase with depth. (*A*) In penetrations through the 5.5-kHz region of the nucleus laminaris, mean phase angles of ipsilateral afferents increased with depth as measured from the floor of the fourth ventricle. The average change in mean phase is about 160 μsec over 700 μm in the nucleus laminaris. Each regression line has a correlation coefficient greater than 0.75. Each penetration is represented by a different symbol. (*B*) Similar but opposite shifts in mean phase occurred in contralateral afferents of the same 5.5-kHz region. In four penetrations, mean phase angles decreased with depth with an average change of 160 μsec over 700 μm in the nucleus laminaris (correlation coefficients greater than 0.81). (*C*) In a single penetration through the 6.0-kHz region of the nucleus laminaris, the delay of phase-locked spikes from the contralateral side (○) decreased with depth (slope of contralateral plot = -0.68 degree/μm, $r = 0.87$), while the delay of the phase-locked spikes increased to stimulation of the ipsilateral ear (●) (slope of ipsilateral plot = 0.46 degree/μm, $r = 0.91$). Note that the two regression lines cross at a depth of about 1300 μm.

isofrequency laminae. These findings led to the hypothesis that interaural time differences are measured and mapped in the nucleus laminaris. The above approach, however, could not identify the neuronal substrate for the systematic distribution of conduction delays.

The present work provides the cellular basis for all of the above findings. Our results show orderly shifts in the arrival of phase-locked spikes with recording depth. Although such shifts would be expected as a consequence of conduction time in a single afferent fiber, the probability of recording from more than one site along a single axon is neglible. Orderly changes in delay with depth were observed in spite of sampling different fibers at different depths. We also found that the maximal delay is similar for all frequencies and that delays are aligned across different isofrequency laminae. These findings show that conduction delays are precisely regulated and mapped in the nucleus laminaris.

We argue that the axonal delay lines described above are a sufficient mechanism for the mapping of time by the nucleus laminaris. Neurons of this nucleus are studded with large somatic spines and very short thick dendrites (19). With this neuronal morphology, conduction delays are unlikely to be produced in the postsynaptic neurons. The presence of delay lines outside the nucleus laminaris is unlikely, because systematic changes in conduction delay appear to occur only within the nucleus laminaris. Shifts of mean phase occur outside the laminaris, but orderly changes in phase are restricted to the dorsoventral axis of the nucleus. This observation is consistent with that made with field potentials, which also showed systematic changes in delay only within the nucleus. Thus the nucleus laminaris contains a dorsoventrally directed map of interaural time differences. In the chick, the nucleus laminaris is a mediolaterally oriented monolayer of cells, and it is therefore impossible that interaural time differences be mapped along the dorsoventral axis. The innervation pattern suggests a mediolateral gradient of delays (17, 18). The monolayer form of the nucleus laminaris represents the plesiomorphic state, because it occurs in reptiles (21) and many birds. The development of the barn owl's pattern from this primitive form is of considerable interest.

In conclusion, we show the neural basis of delay lines, and we suggest how they are used for the measurement of interaural time differences. The arrival of phase-locked spikes at a particular locus in the nucleus laminaris varies systematically as a function of distance from either surface of the nucleus. Each locus in the nucleus laminaris can be characterized by a pair of delays obtained for ipsi- and contralateral fibers, and phase-locked spikes arrive at a laminaris cell with delays unique to its locus. If a laminaris cell works as a coincidence detector (8), spikes from the two sides arrive at the cell simultaneously only when the difference between the ipsi- and contra delays is eliminated. This condition can be met by the imposition of an acoustic delay or advance that is equal in magnitude but opposite in sign to the disparity in transmission time imposed by unequal paths. Different interaural time disparities are required to fire cells at different depths, which leads to the hypothesis that the nucleus laminaris contains a neuronal map of interaural time difference. The use of phase-locked spikes, however, creates an ambiguity in encoding interaural time differences. Spikes arriving n periods apart signal the same time because the auditory system does not count cycles. Consequently, laminaris neurons respond not only to a particular interaural time difference Δt or "characteristic delay" (22) but also to $\Delta t + nT$, where n is an integer and T is the period of the stimulus tone or the best frequency of the neuron (8). Hence, we hypothesize that characteristic delays are mapped along the dorsoventral axis of the nucleus laminaris. Finally, it should be pointed out that the neural delays observed are consistent with the behaviorally relevant range of interaural time differences (6).

We thank Ted Sullivan and Larry Proctor for advice and the use of data analysis programs, and Ted Bullock, Walter Heiligenberg, Eric Knudsen, Andy Moiseff, Terry Takahashi, Susan Volman, and Hermann Wagner for reading this manuscript. This work was supported by National Institutes of Health Grant NS14617 to M.K. and National Research Service Award NS07475 to C.E.C.

1. Jeffress, L. A. (1948) *J. Comp. Physiol. Psychol.* **41**, 35–39.
2. Liklider, J. & Webster, J. C. (1950) *J. Acoust. Soc. Am.* **22**, 191–195.
3. Cherry, E. C. & Sayers, B. (1956) *J. Acoust. Soc. Am.* **28**, 889–895.

4. Goldberg, J. M. & Brown, P. B. (1969) *J. Neurophysiol.* **32,** 613–636.
5. Yin, T. C. T., Chan, J. C. K. & Carney, L. H. (1987) *J. Neurophysiol.* **58,** 562–583.
6. Moiseff, A. & Konishi, M. (1981) *J. Neurosci.* **1,** 40–48.
7. Moiseff, A. & Konishi, M. (1983) *J. Neurosci.* **3,** 2553–2562.
8. Sullivan, W. E. & Konishi, M. (1986) *Proc. Natl. Acad. Sci. USA* **83,** 8400–8404.
9. Bennett, M. V. L. (1971) in *Fish Physiology,* eds. Hoar, W. S. & Randall, D. J. (Academic, New York), Vol. 5, pp. 347–491.
10. Waxman, S. G., ed. (1978) *Physiology and Pathology of Axons* (Raven, New York).
11. Adams, J. C. (1981) *J. Histochem. Cytochem.* **29,** 775.
12. Takahashi, T. & Konishi, M. (1988) *J. Comp. Neurol.* **274,** 190–211.
13. Sereno, M. (1985) *J. Comp. Neurol.* **233,** 48–90.
14. Sullivan, W. E. & Konishi, M. (1984) *J. Neurosci.* **4,** 1787–1799.
15. Boord, R. L. & Rasmussen, G. L. (1963) *J. Comp. Neurol.* **120,** 463–475.
16. Jhaveri, S. & Morest, D. K. (1982) *Neuroscience* **7,** 809– 835.
17. Parks, T. N. & Rubel, E. W. (1975) *J. Comp. Neurol.* **164,** 435–448.
18. Young, S. R. & Rubel, E. W. (1983) *J. Neurosci.* **3,** 1373–1378.
19. Carr, C. E., Brecha, N. & Konishi, M. (1985) *Neurosci. Abstr.* **11,** 735.
20. Carr, C. E. (1986) *Brain Behav. Evol.* **238,** 122–133.
21. Leake, P. A. (1974) *Brain Behav. Evol.* **5,** 170–196.
22. Rose, J. E., Grass, N. G., Geisler, C. D. & Hind, J. E. (1966) *J. Neurophysiol.* **29,** 288–314.